Environment and Natural Resources Journal 2021; 19(4): 255-265

Effectivity of Indonesian Rice Husk as an Adsorbent for Removing Congo Red from Aqueous Solutions

Neza Rahayu Palapa[1], Normah[2], Tarmizi Taher[3], Risfidian Mohadi[1,2], Addy Rachmat[1,2], and Aldes Lesbani[1,4*]

[1]Graduate School of Mathematics and Natural Sciences, Univesitas Sriwijaya, Palembang, South Sumatera 30139, Indonesia
[2]Department of Chemistry, Faculty of Mathematics and Natural Sciences, Universitas Sriwijaya, Ogan Ilir, South Sumatera 30662, Indonesia
[3]Department of Environmental Engineering, Institut Teknologi Sumatera, Kecamatan Jati Agung, Lampung Selatan 35365, Indonesian
[4]Reseach Center of Inorganic Materials and Complexes, Universitas Sriwijaya, Ogan Ilir, South Sumatera 30662, Indonesia

ARTICLE INFO

Received: 13 Oct 2020
Received in revised: 15 Dec 2020
Accepted: 28 Jan 2021
Published online: 17 May 2021
DOI: 10.32526/ennrj/19/2020232

Keywords:
Low-cost adsorbent/ Biomass/ Congo red/ Adsorption process/ Dyes

*** Corresponding author:**
E-mail:
aldeslesbani@pps.unsri.ac.id

ABSTRACT

Indonesian rice husk biochar (RH-BC) was prepared by pyrolysis method at 500°C and characterized using X-ray diffraction, Fourier-transform infrared spectroscopy, surface-area-specific analysis by Brunauer-Emmett-Teller, and scanning electron microscopy. The RH-BC were used as adsorbents for enhancing the adsorption of Congo red compared to pristine rice husk (RH) in aqueous solutions. The results of characterization through surface-area-specific analysis showed the surface area of RH-BC (72.25 m^2/g) was ten times higher than RH (7.08 m^2/g) owing to high-temperature treatment. The results of the adsorption study showed that the RH and RH-BC followed the pseudo-second-order kinetic model and the Freundlich isotherm equation with maximum adsorption capacities of 85.470 mg/g and 72.993 mg/g for the RH-BC and RH, respectively. The thermodynamic parameters of adsorption indicated spontaneous and endothermic processes. The reusability of the adsorbents (RH and RH-BC) showed that they are potentially suitable for extracting Congo red from aqueous solution up to three adsorption-desorption cycles. Their performance sharply decreases after the fourth and fifth cycles.

1. INTRODUCTION

Indonesia has many industries, such as plastics, textiles, pulps, papers, pharmaceuticals, and cosmetics that produce waste pollutants, such as dyes, that are released into the environment. The presence of dyes in aquatic systems can cause severe environmental problems (Saini, 2017; Vinsiah et al., 2017; Malik et al., 2020) These dyes are carcinogenic, non-biodegradable, and toxic to humans and biota in environmental systems (Hassaan and Nemr, 2017; Yaseen and Scholz, 2019). Several methods for removing dyes from wastewater have been developed to decrease their impact on health and environment (Banerjee and Chattopadhyaya, 2017). These methods include adsorption (Palapa et al., 2021), coagulation/ flocculation (Mozumder and Islam, 2010), electrochemical (Cotillas et al., 2018), microbial decomposition (Patil et al., 2016), sonochemical (Gholami et al., 2019), wet air oxidation, ozonation (Banerjee and Chattopadhyaya, 2017), and ion exchange (Choi et al., 2020).

Among these methods, adsorption is a well-known separation method that provides an effective process for dye removal from wastewater. The adsorption performance is based on the properties of the adsorbent materials. (Han et al., 2008; Banerjee and Chattopadhyaya, 2017). Several adsorbents have been tested for dye removal from wastewater, such as activated zeolites, clays, bentonite, chitin, chitosan, cellulose, algae, and carbon-based materials (Kandisa et al., 2016; Momina et al., 2018; Boulaiche et al., 2019; Rabie et al., 2020).

Activated carbon is an effective adsorbent for dye removal; however, the high cost of activated carbon limits its application (Azargohar and Dalai, 2006). Recently, agricultural wastes, such as orange

Citation: Palapa NR, Normah, Taher T, Mohadi R, Rachmat A, Lesbani A. Effectivity of Indonesian rice husk as an adsorbent for removing Congo red from aqueous solutions. Environ. Nat. Resour. J. 2021;19(4):255-265 (https://doi.org/10.32526/ennrj/19/2020232)

peel (Annadurai et al., 2002), longan peel (Wang et al., 2016), limetta peel (Shakoor and Nasar, 2016), and rice husk (RH) (Liu and Zhang, 2009), have been used as feedstock for adsorbents. RH is agricultural waste feedstock produced from the rice milling industry, and it contains chemical compounds, such as lignin, cellulose, and hemicellulose, which can be used as active-site adsorbents for dye removal (Connor et al., 2018). However, the RH has a low adsorption capacity. Thus, to increase this adsorption capacity, they should be activated by carbonization (Bamroongwongdee et al., 2019; Milla et al., 2013).

Malik et al. (2020) also reported comparative comparison of RH, RH char, and chemically modified RH used as adsorbents for the removal of the Congo red dye. This study reported that the adsorption capacities of the RH, RH char, and chemically modified RH char (CMRHC) are 1.58 mg/g, 1.28 mg/g, and 2.04 mg/g, respectively, for Congo red dye removal. This comparative study indicated that the adsorption efficiency of the CMRHC was higher than that of the RH and RH char. Herlina and Masri (2017) reported that the adsorption of Congo red using the RH occurred in an optimum contact time of 30 min, with an adsorption percentage of 91.99%. The adsorption capacity was 7.19 mg/g. Gad et al. (2016) also used the RH as an adsorbent of metal ion Co(II) from wastewater, which resulted in a maximum adsorption capacity of 75.70 mg/g, and it followed the Langmuir isotherm model.

In this study, the RH and RH-BC-based local Indonesian feedstock were used as adsorbents of Congo red from aqueous solutions. The factors influencing the adsorption process, such as adsorption time, concentration of Congo red, and temperature adsorption, were studied in detail. The kinetics of adsorption, isotherm, and thermodynamics of the adsorption process of Congo red onto the RH and RH-BC are discussed in this article.

2. METHODOLOGY

2.1 Chemical and instrumentation

Analytical grade (p.a.) chemicals such as sodium hydroxide, ethanol, hydrochloric acid, and congo red (>75%) were purchased from Merck (Darmstadt, Germany). Water was supplied by the Research Center of Inorganic Materials and Complexes, FMIPA Universitas Sriwijaya. Destilled water was obtained after purify using a Pureit®, which removed undesirable ionic, organic, and bacterial contaminants from the water. Further, this water was prepared for washing the RH from rice mills in Bukataorganics, Indonesia. The RH was washed with distilled water and dried at 60°C in an oven for 8 h. Production of the RH-BC by pyrolysis method was done by placing RH in the reactor and then heating at 600°C for 1 h. The RH and RH-BC was characterized using X-ray diffraction (XRD; Rigaku miniflex-6000). The RH and RH-BC were scanned from 5° to 80° at a scan rate of 1° min^{-1}. The functional groups were analyzed using Fourier-transform infrared (FT-IR) spectroscopy (Shimadzu Prestige-21) at 400-4,000 cm^{-1} and a KBr pellet. The adsorption-desorption of N_2 was performed using a Quantachrome Micrometic ASAP adsorption analyzer. Morphology analysis was performed using a scanning electron microscopy (SEM; Quanta-650 Oxford). The concentration of Congo red was determined through an ultraviolet-visible (UV-Vis) spectrophotometer (Biobase BK-UV 1800 PC) at 501 nm.

2.2 Adsorption process

The adsorption process was studied in a batch system by varying the adsorption time, Congo red concentration, and temperature for three replication measurements. The initial pH of Congo red is 5.3, and the adsorbents were sieved through 80 mesh. The variation in the adsorption times was performed with 50 mg/L of Congo red dye. Further, 25 mL of the Congo red dye was placed in a glass beaker, 0.025 g of the adsorbent was added to it, and the mixture was stirred by a horizontal shaker for 5-180 min at 250 rpm. The mixing solution was centrifuged at 1,000 rpm before scanning at 501 nm using a UV-Vis spectrophotometer. The kinetic adsorption was calculated using the kinetic adsorption models, such as pseudo-first-order (PFO) and pseudo-second-order (PSO) kinetic models, as presented in equations 1 and 2.

$$\log (q_e - q_t) = \log q_e - \left(\frac{k_1}{2{,}303}\right) t \quad (1)$$

$$\frac{t}{qt} = \frac{1}{k_2 qe^2} + \frac{1}{qe} t \quad (2)$$

Where; q_e is the adsorption capacity at equilibrium (mg/g); q_t is the adsorption capacity (mg/g) at t, which is the adsorption time (min); k_1 and k_2 denote the adsorption kinetic rates at PFO kinetics (min^{-1}) and PSO kinetics (g/mg·min), respectively.

The Congo red concentration was determined at dye concentrations of 50, 75, 100, 125, and 150 mg/L using 0.025 g of the adsorbents and 25 mL of Congo

red. Moreover, the mixture was stirred by a horizontal shaker for 100 min at 250 rpm at different adsorption temperatures of 303, 313, 323, and 333 K. The concentration of the Congo red was analyzed using the UV-Vis spectrophotometer at a maximum wavelength of 501 nm. Thereafter, the thermodynamic parameters were obtained from the Langmuir and Freundlich equations. The Langmuir adsorption model is assumed to be the chemical and monolayer adsorption processes, while the Freundlich adsorption model is assumed to be the physical and multilayer adsorption processes. Equations 3, 4, and 5 represent the Langmuir adsorption model, Freundlich adsorption model, and thermodynamic equations, respectively.

$$\frac{C}{m} = \frac{1}{bK_{ML}} + \frac{C}{b} \quad (3)$$

Where; C is the saturated concentration of the adsorbate, m is the amount of adsorbate, b is the maximum adsorption capacity (mg/g), and K_{ML} is the Langmuir constant (L/mg).

$$\text{Log } q_e = \log K_F + 1/n \log C_e \quad (4)$$

Where; q_e is the adsorption capacity at equilibrium (mg/g), C_e is the concentration of adsorbate at equilibrium (mg/L), and K_F is the Freundlich constant.

$$\ln K_d = \frac{\Delta S}{R} - \frac{\Delta H}{RT} \quad (5)$$

Where; R is the rate gas constant, T is the temperature of the adsorption process (K), K_d is the thermodynamic equilibrium constant, ΔH is the enthalpy (kJ/mol), and ΔS is the entropy (J/mol·K).

2.3 Desorption and reusability process

Based on the amount of adsorbed dye, the amount of desorbed dye can be calculated using the following equation.

$$\%\ D = \frac{C_{ads}}{C_{dsp}} \times 100\% \quad (6)$$

Where; C_{ads} is the concentration of adsorbed Congo red (mg/L), C_{dsp} is the concentration of desorbed Congo red (mg/L), and %D is the percentage of the desorption process.

The regeneration efficiency is determined using the equation:

$$\%\ \text{regeneration} = \frac{Q_r}{Q_0} \times 100\% \quad (7)$$

Where; Q_r is the adsorption capacity of reusability (mg/g) and Q_o is the adsorption capacity of the initial reusability (mg/g).

The desorption process was used to test each adsorbent using 1 g of RH and RH-BC, followed by the addition of 50 mL of the Congo red solution. Then, the mixture was stirred for 2 h. The used adsorbent was desorbed by taking 0.01 g of RH and RH-BC, respectively, and adding 10 mL of solvent (sodium hydroxide (0.01 M), hydrochloric acid (0.01 M), absolute ethanol, and distilled water) and stirring the mixture for 2 h for each conical flask. The reusability process was performed with the desorbed adsorbent reused to adsorb 100 mg/L of Congo red. The adsorption was performed for 2 h using a batch system and analyzed by UV-Vis spectrophotometry. The reusability of the adsorbent was evaluated in three cycles of the adsorption process.

3. RESULTS AND DISCUSSION

3.1 Adsorbent characterization

Figure 1 shows the XRD powder patterns of the RH and RH-BC characterization at 2θ diffraction peaks shown in the range of 16°-29°. A previous study (Suyanta and Kuncaka, 2011) reported that there were no diffraction peaks, except one of approximately 23° with reflection (002) at 2θ diffraction. These diffractions indicate the presence of silica in an amorphous state from the RH and RH-BC (Milla et al., 2013). The XRD powder pattern of the RH exhibited diffraction at 23°. Another 2θ peak (101) at 18° disappeared after heating the RH at a high temperature (600°C) due to decomposition of cellulose (Rosa et al., 2012). As reported by De Bhowmick et al. (2018), the change in the peak occurred due to the destruction of the biomass structure by pyrolysis.

The FT-IR spectra of the RH and RH-BC are shown in Figure 2. The vibration peak at 3,448 cm^{-1} corresponds to the -OH group. The peak at 1,620 cm^{-1} indicates the presence of C-O bonds in the carboxylate group. The peak at wavenumber 794 cm^{-1} corresponds to the presence of Si-O bond (Bamroongwongdee et al., 2019). The vibration at 1,103 cm^{-1} refers to C-H stretching of lignin in the RH and RH-BC (Gad et al., 2016). Furthermore, the intensity of the water molecule (OH vibration) and carboxylate group (CO vibration) in the RH decreased after heating at 600°C to form the RH-BC.

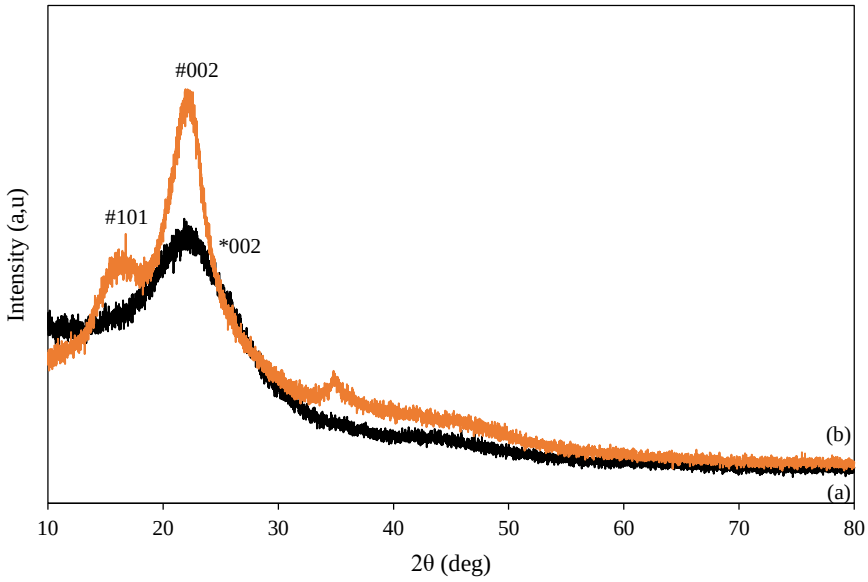

Figure 1. XRD powder patterns of (a) RH-BC and (b) RH

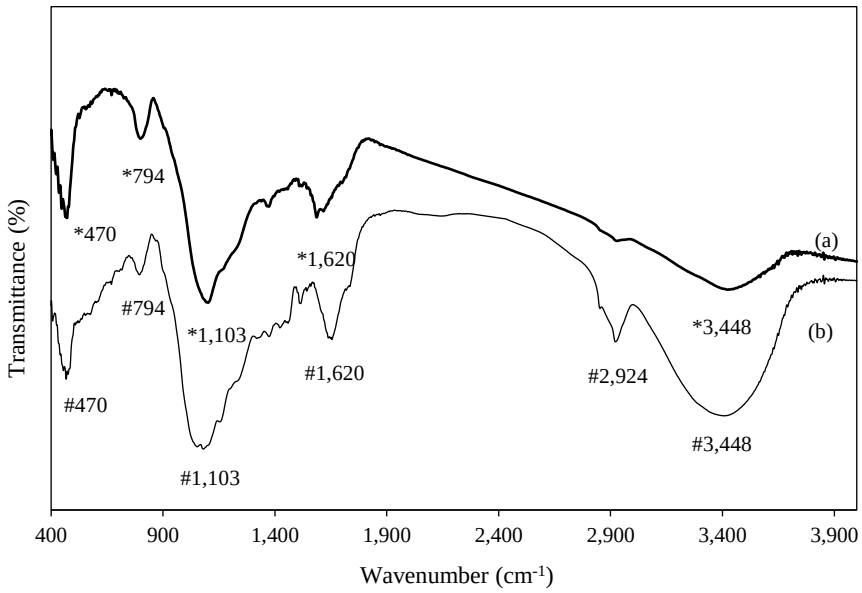

Figure 2. FT-IR spectra of (a) RH-BC and (b) RH

Table 1 shows the Brunauer-Emmett-Teller (BET) surface analyses of the RH and RH-BC. The RH-BC has a larger surface area than that of the RH because of the use of high temperatures during RH-BC pyrolysis. These temperatures can open the pore channels of the RH during thermal process to form the RH-BC (Fernandes et al., 2016). As shown in Table 1, the larger pore size can affect the higher adsorption capacity due to the increasing pore volume. This was also reported by Mangun et al. (1998). They also reported that the pore size and volume size can affect the adsorption capacity.

Table 1. Surface properties of RH and RH-BC

Adsorbent	Surface area (m^2/g)	Pore size (nm)	Pore volume (cm^3/g)
RH-BC	72.25	3.33	0.060
RH	7.08	3.14	0.011

SEM-energy-dispersive X-ray (EDX) analysis revealed the elemental composition of the RH and RH-BC. The SEM-EDX analyses of the RH and RH-BC are shown in Figure 3(a) and 3(b), respectively. The morphology of the RH (Figure 3(a)) shows a uniform

size with a round stem shape. However, the RH-BC has an irregular pore size, as shown in Figure 3(b) (Leng et al., 2015). As expected from the results of the BET analysis, the opening of pores increases the surface area of the RH-BC. Furthermore, the EDX results showed that both the RH-BC and RH contain C, Si, O, S, P, N, and Al. The main contents of the RH are C, O, and Si, which are obtained from SiO_2 and the carboxylate groups. The main components of the RH-BC are C and Si. The elements Al, P, S, and N are obtained through plants as non-essential elements (Wang et al., 2017).

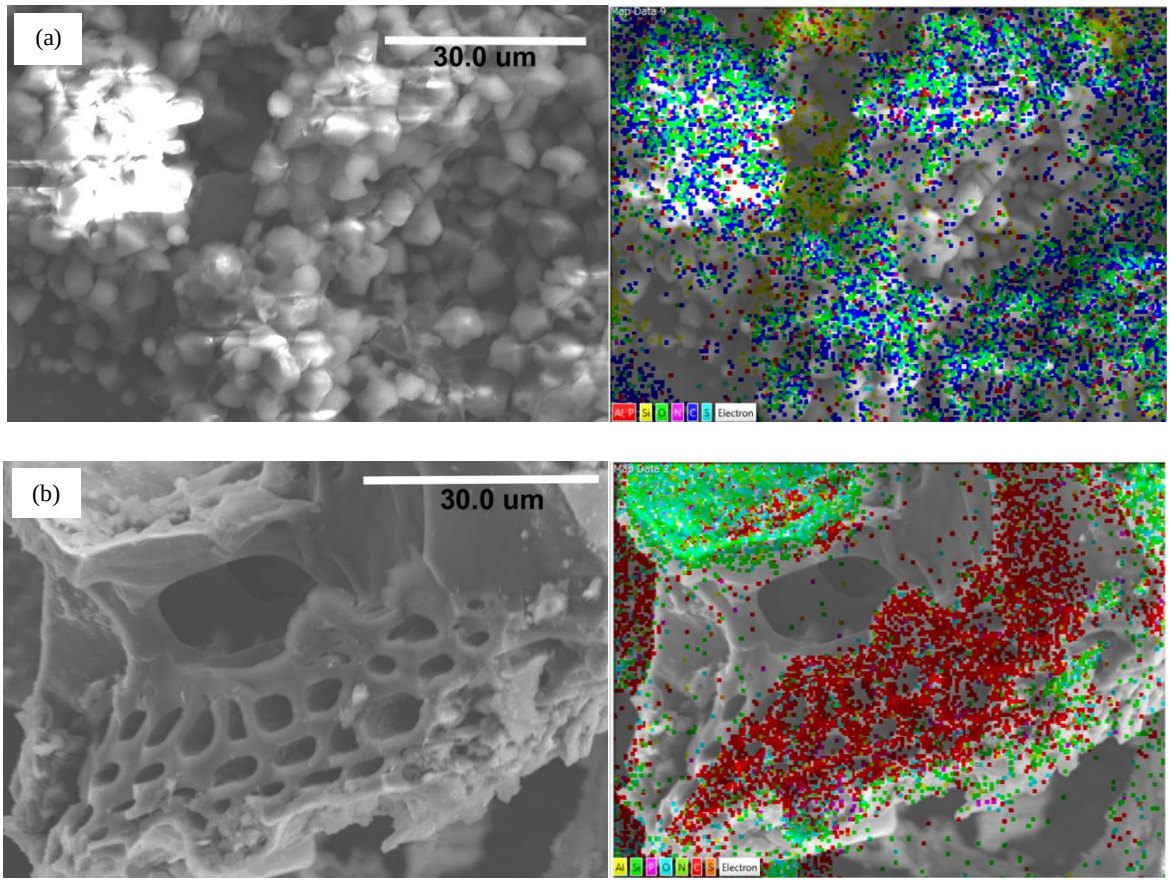

Figure 3. SEM-EDX analysis of (a) RH and (b) RH-BC

3.2 Adsorption study

The RH and RH-BC were used as adsorbents for the adsorption of Congo red from aqueous solutions. First, the adsorption was studied based on the adsorption time, as shown in Figure 4 and Table 2. The adsorption of Congo red on the RH and RH-BC increased sharply with the increasing adsorption time for both the adsorbents, and it reached equilibrium after 100 min of adsorption. The adsorption time data were calculated to obtain the kinetic parameters using the PFO and PSO kinetic models, as described by Equations 1 and 2. The adsorption of Congo red follows the PSO kinetic model, with a correlation coefficient R^2>0.995. The RH-BC has a larger adsorption capacity (31.619 mg/g) than that of the RH (22.008 mg/g) because of its large surface area, which indicates sorbent-sorbate electrostatic attraction. According to Bamroongwongdee et al. 2019 the PSO kinetic model also confirmed that the adsorption process involves a chemisorption stage, which constitutes the rate-limiting process.

Second, the effects of the Congo red concentration and temperature on the equilibrium of the adsorption process were studied. Figure 5 shows the difference in the Congo red concentration and adsorption temperature in the case of RH and RH-BC. The figure also shows that the adsorption capacity increases with increasing temperature of the adsorption process.

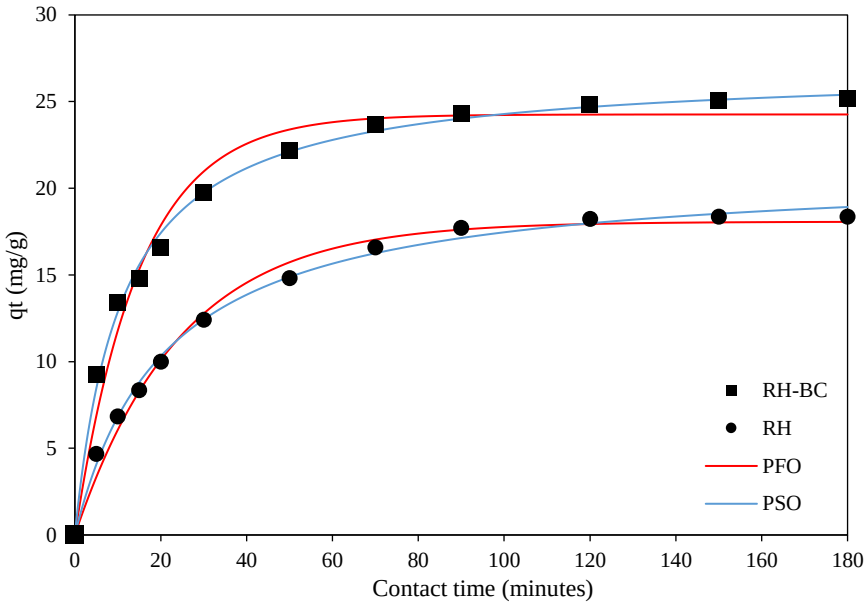

Figure 4. The plot of the fitted kinetics model against the experimental data

Table 2. Kinetic adsorption of Congo red on the RH and RH-BC

Adsorbent	Initial concentration (mg/L)	$Qe_{experiment}$ (mg/g)	PFO			PSO		
			Qe_{Calc} (mg/g)	R^2	k_1	Qe_{Calc} (mg/g)	R^2	k_2
RH-BC	51.492	31.619	29.573	0.995	0.032	36.231	0.997	0.023
RH	51.492	22.008	19.037	0.979	0.029	25.062	0.994	0.021

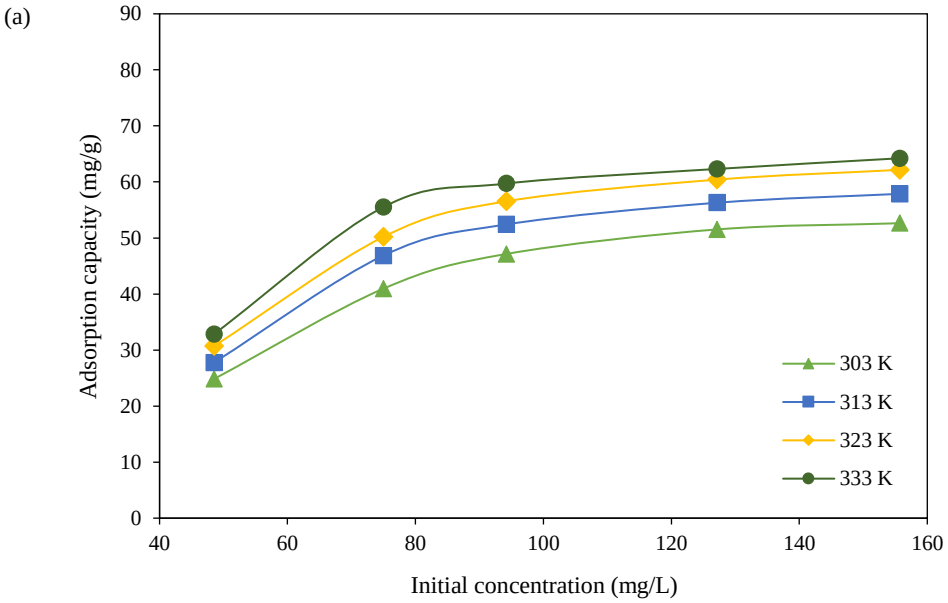

Figure 5. Effects of Congo red dye concentration on the adsorption capacities of (a) RH and (b) RH-BC

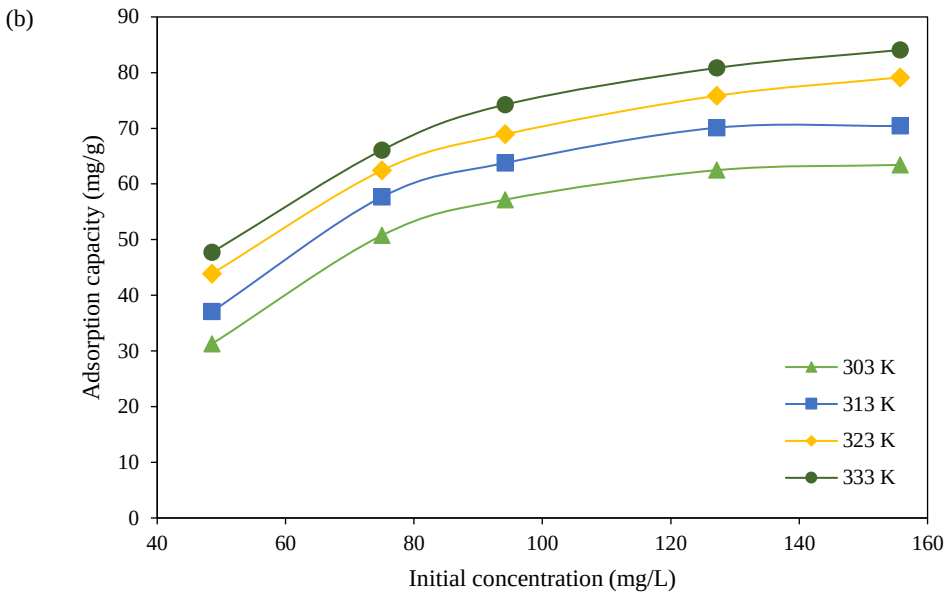

Figure 5. Effects of Congo red dye concentration on the adsorption capacities of (a) RH and (b) RH-BC (cont.)

Table 3 presents the Langmuir and Freundlich data, which were obtained from the data provided in Figure 5. According to the data in Table 3, the adsorption on the RH and RH-BC is appropriate with the Freundlich isotherm model with R^2>0.99, which suggests that the adsorption process is physisorption and occurs through multilayer (Wijayanti et al., 2018). However, this is in contrast to the PSO equation, which indicated that the adsorption process involves chemisorption. This finding suggests that physico-chemical adsorption occurred in the adsorption process. This conforms with the enthalpy results listed in Table 4, which indicate that the adsorption of Congo red has low enthalpy. Further, according to IUPAC, physisorption with the enthalpy in the range of 4-40 kJ/mol and >40 kJ/mol corresponds to chemisorption (Thommes et al., 2015; Oktriyanti et al., 2019). The increasing dye uptake with the increasing temperature decreased the viscosity of the solution, increased the porosity, or interlayer, resulting in the enhancement of active sites form (Zhu et al., 2005). According to the results summarized in Table 4, the adsorption capacity of Congo red removal using the RH-BC is slightly higher than that for other adsorbents.

Table 3. Isotherm models of Congo red adsorption on RH and RH-BC

	Isotherm	Parameters	303 K	313 K	323 K	333 K
RH-BC	Langmuir	Qmax	77.519	79.365	83.333	85.470
		k_L	0.058	0.112	0.219	0.480
		R^2	0.971	0.992	0.999	0.998
	Freundlich	n	1.909	4.361	1.448	1.444
		k_F	7.034	1.328	3.631	3.928
		R^2	0.999	0.996	0.993	0.999
RH	Langmuir	Qmax	60.606	72.993	74.627	75.188
		k_L	0.067	0.088	0.039	0.058
		R^2	0.997	0.976	0.956	0.969
	Freundlich	N	1.071	10.953	5.688	9.497
		k_F	1.295	1.455	1.386	1.441
		R^2	0.999	0.979	0.983	0.994

Table 4. Comparison of Congo red adsorption using different adsorbents.

Adsorbent	Qe (mg/g)	Refs
Na-bentonite	35.84	(Vimonses et al., 2009)
Bagasse fly ash	11.88	(Mall et al., 2005)
Spirulinna algae	3.11	(Mohadi et al., 2017)
m-cell/Fe_3O_4/ACCs	66.09	(Zhu et al., 2011)
Magnetic Fe_3O_4@graphene	33.66	(Inyang et al., 2012)
Funalia trogii	83.70	(Bayramoglu and Arica, 2018)
RH-BC	85.47	This research
RH	75.188	This research

The thermodynamic parameters of the Congo red adsorption on the RH and RH-BC adsorbents, such as ΔH (enthalpy), ΔG (Gibbs free energy), and ΔS (entropy), are shown in Table 5. The positive values of ΔS indicate an increase in the degree of irregularity between the adsorbate and adsorbent. The positive value of ΔH indicates that the Congo red adsorption on the RH and RH-BC is endothermic. The negative value of ΔG indicates that the Congo red adsorption is spontaneous (Naushad et al., 2019).

Table 5. Thermodynamic parameters of Congo red adsorption on RH and RH-BC

Concentration	T (K)	Q_e (mg/g)	ΔH (kJ/mol)	ΔS (kJ/mol)	ΔG (kJ/mol)
48.524 mg/L	303	31.270	9.544	3.200	-0.070
	313	37.063			-0.387
	323	43.889			-0.704
	333	47.698			-1.022
48.524 mg/L	303	24.841	19.565	6.500	-0.132
	313	27.778			-0.782
	323	30.714			-1.432
	333	32.857			-2.082

Desorption of the adsorbent was studied using several solvents on the RH and RH-BC after the adsorption of Congo red, and the results are shown in Figure 6, which indicate that hydrochloric acid as a solvent can give higher results in the desorption process of Congo red. This is because the H^+ ion from the hydrochloric acid releases the Congo red dye anion by interacting with the adsorbent. Congo red prefers

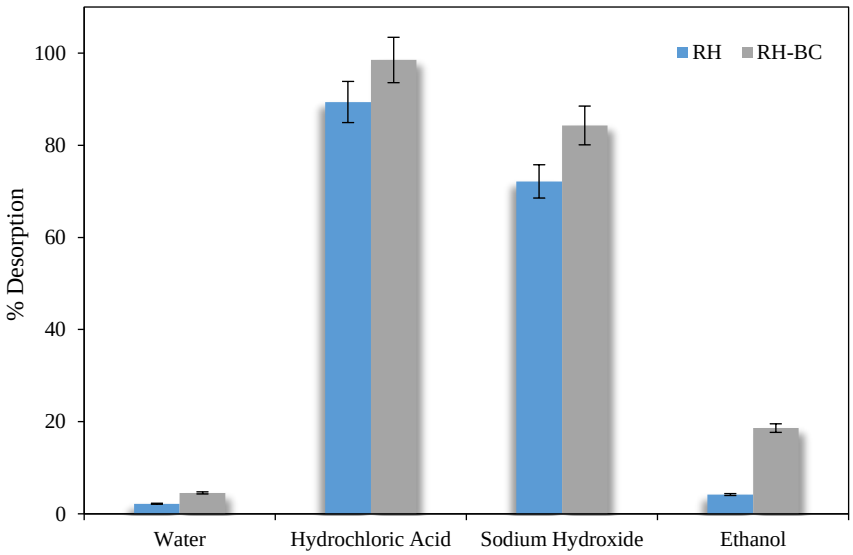

Figure 6. Desorption of Congo red on the RH and RH-BC

lower number of H^+ ions than those present in hydrochloric acid because of greater electrostatic interactions than adsorbents (Palapa et al., 2020). The reusability of the adsorbent was evaluated using hydrochloric acid as a desorption reagent to release Congo red after the adsorption process.

The reusability study was conducted for five adsorption cycles, as demonstrated in Figure 7. The adsorption capacity of Congo red on both the adsorbents decreased sharply after three cycles, i.e., during the fourth and fifth adsorption processes. The first reusabilities of the RH and RH-BC were 58.88% and 54.32%, and the second reusabilities were 53.44% and 47.33% for the RH and RH-BC, respectively. The third reusability was more stable with reusability values of 47.91% for RH and 44.24% for RH-BC. However, the adsorption capacity decreased significantly in the fourth and fifth adsorption processes. Thus, the RH and RH-BC are suitable adsorbents for the Congo red adsorption in three adsorption cycles. Furthermore, these adsorbents can be reused, although their adsorption capacity is slightly reduced.

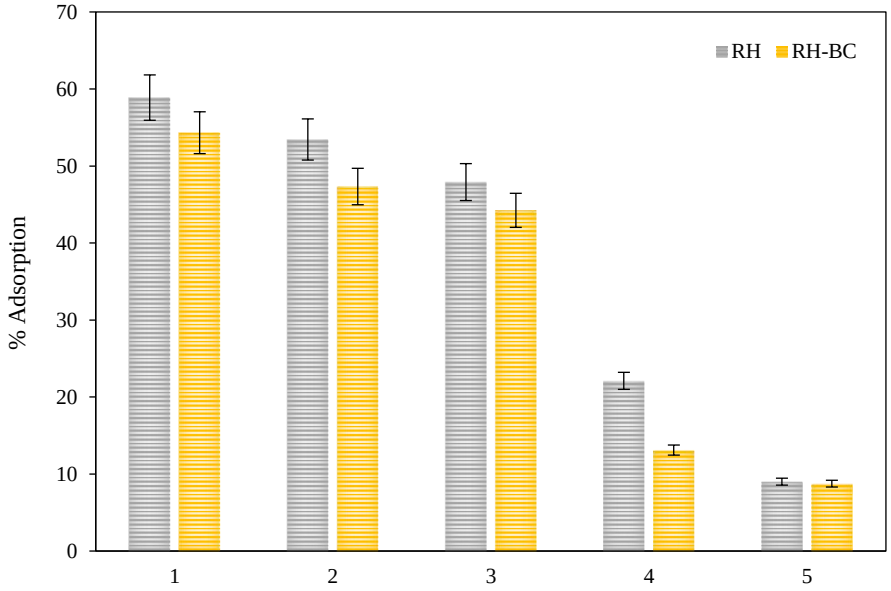

Figure 7. Reusability of the RH and RH-BC for Congo red adsorption

4. CONCLUSION

In this study, characterization of RH and RH-BC using XRD indicated the presence of silica molecules at a diffraction peak of 23°. The FT-IR spectra of the RH and RH-BC showed Si-O vibrations at 794 cm^{-1}, and the peak at 1,103 cm^{-1} corresponded to the C-H strain, which indicated the presence of lignin on the RH and RH-BC. The BET analysis showed that the surface areas of the RH and RH-BC were 72.25 m^2/g and 7.08 m^2/g, respectively. The adsorption of Congo red on the RH and RH-BC followed the PSO kinetics model with optimum adsorption after 100 min and the Freundlich equation model with a maximum adsorption capacity of 85.470 mg/L. The RH-BC was more effective at Congo red dye removal than the RH. The thermodynamic parameters indicated that the Congo red was adsorbed spontaneously on the RH and RH-BC, and this adsorption was an endothermic process. The reusability of the adsorbents indicated that the RH and RH-BC had a decreasing adsorption capacity after three cycles of adsorption. Furthermore, these experimental results are useful to increase the use of biomass as a potential adsorbent for wastewater treatment. The studied adsorbents are suitable to remove Congo red in an aqueous solution. In addition, the use of agricultural wastes as one source of adsorbents has the potential to further help to reduce agricultural waste in the environment.

ACKNOWLEDGEMENTS

This study was supported by “Hibah Profesi” Universitas Sriwijaya in fiscal year 2020-2021 by the financial support program for research with contact number 0687/UN9/SK.BUK.KP/2020. Special thanks for Research Center of Inorganic Materials and Complexes, Faculty of Mathematic and Natural

Science, Universitas Sriwijaya for analysis and instrumental measurement.

REFERENCES

Annadurai G, Juang RS, Lee DJ. Use of cellulose-based wastes for adsorption of dyes from aqueous solutions. Journal of Hazardous Materials 2002;92(3):263-74.

Azargohar R, Dalai AK. Biochar as a precursor of activated carbon. Applied Biochemistry and Biotechnology 2006;129-132:762-73.

Bamroongwongdee C, Suwannee S, Kongsomsaksiri M. Adsorption of Congo red from aqueous solution by surfactant-modified rice husk: Kinetic, isotherm and thermodynamic analysis. Songklanakarin Journal of Science and Technology 2019;41(5):1076-83.

Banerjee S, Chattopadhyaya MC. Adsorption characteristics for the removal of a toxic dye, tartrazine from aqueous solutions by a low cost agricultural by-product. Arabian Journal of Chemistry 2017;10:S1629-38.

Bayramoglu G, Arica MY. Adsorption of Congo red dye by native amine and carboxyl modified biomass of *Funalia trogii*: Isotherms, kinetics and thermodynamics mechanisms. Korean Journal of Chemical Engineering 2018;35:1303-11.

De Bhowmick G, Sarmah AK, Sen R. Production and characterization of a value added biochar mix using seaweed, rice husk and pine sawdust: A parametric study. Journal of Cleaner Production 2018;200:641-56.

Boulaiche W, Hamdi B, Trari M. Removal of heavy metals by chitin: Equilibrium, kinetic and thermodynamic studies. Applied Water Science 2019;9:39.

Choi Y, Gurav R, Kim HJ, Yang Y, Bhatia SK. Evaluation for simultaneous removal of anionic and cationic dyes onto maple leaf-derived biochar using response surface methodology. Applied Sciences 2020;10:2982.

Connor DO, Peng T, Li G, Wang S, Duan L, Mulder J, et al. Sulfur-modified rice husk biochar: A green method for the remediation of mercury contaminated soil. Science of the Total Environment 2018;621:819-26.

Cotillas S, Llanos J, Cañizares P, Clematis D, Cerisola G, Rodrigo MA, et al. Removal of Procion red MX-5B dye from wastewater by conductive-diamond electrochemical oxidation. Electrochimica Acta 2018;263:1-7.

Fernandes IJ, Calheiro D, Kieling AG, Moraes CAM, Rocha TLAC, Brehm FA, et al. Characterization of rice husk ash produced using different biomass combustion techniques for energy. Fuel 2016;165:351-9.

Gad HM, Omar H, Aziz A, Hassan M, Khalil M. Treatment of rice husk ash to improve adsorption capacity of cobalt from aqueous solution. Asian Journal of Chemistry 2016;28(2):385-94.

Gholami P, Dinpazhoh L, Khataee A, Hassani A, Bhatnagar A. Facile hydrothermal synthesis of novel Fe-Cu layered double hydroxide/biochar nanocomposite with enhanced sonocatalytic activity for degradation of cefazolin sodium. Journal of Hazardous Materials 2019;381:120742.

Han R, Ding D, Xu Y, Zou W, Wang Y, Li Y, et al. Use of rice husk for the adsorption of congo red from aqueous solution in column mode. Bioresource Technology 2008;99(8):2938-46.

Hassaan MA, Nemr A El. Health and environmental impacts of dyes: Mini review. American Journal of Environmental Science and Engineering 2017;1(3):64-7.

Herlina R, Masri MS. Adsorption study of rice bran against Congo red dyes in Wajo. Journal Chemical 2017;18(1):16-25.

Inyang M, Gao B, Yao Y, Xue Y, Zimmerman AR, Pullammanappallil P, et al. Removal of heavy metals from aqueous solution by biochars derived from anaerobically digested biomass. Bioresource Technology 2012;110:50-6.

Kandisa RV, Kv NS, Shaik KB, Gopinath R. Dye removal by adsorption: A review. Journal of Bioremediation and Biodegradation 2016;7(6):371.

Leng L, Yuan X, Zeng G, Shao J, Chen X, Wu Z, et al. Surface characterization of rice husk bio-char produced by liquefaction and application for cationic dye (Malachite green) adsorption. Fuel 2015;155:77-85.

Liu Z, Zhang FS. Removal of lead from water using biochars prepared from hydrothermal liquefaction of biomass. Journal of Hazardous Materials 2009;167(1-3):933-9.

Malik A, Khan A, Natasha A, Naeem M. A comparative study of the adsorption of Congo red dye on rice husk, rice husk char and chemically modified rice husk char from aqueous media. Bulletin of the Chemical Society of Ethiopia 2020; 34(1):41-54.

Mall ID, Srivastava VC, Agarwal NK, Mishra IM. Adsorptive removal of malachite green dye from aqueous solution by bagasse fly ash and activated carbon-kinetic study and equilibrium isotherm analyses. Colloids and Surfaces A: Physicochemical and Engineering Aspects 2005;264(1-3): 17-28.

Mangun CL, Daley MA, Braatz RD, Economy J. Effect of pore size on adsorption of hydrocarbons in phenolic-based activated carbon fibers. Carbon 1998;36(1-2):123-9.

Milla OV, Rivera EB, Huang W, Chien C, Wang Y. Agronomic properties and characterization of rice husk and wood biochars and their effect on the growth of water spinach in a field test. Journal of Soil Science and Plant Nutrition 2013;13(2):251-66.

Mohadi R, Hanafiah Z, Hermansyah H, Zulkifli H. Adsorption of procion red and congo red dyes using microalgae *Spirulina* sp. Science and Technology Indonesia 2017;2(4):102-4.

Momina, Shahadat M, Isamil S. Regeneration performance of clay-based adsorbents for the removal of industrial dyes: A review. RSC Advances 2018;8:24571-87.

Mozumder MSI, Islam MA. Development of treatment technology for dye containing industrial wastewater. Journal of Scientific Research 2010;2(3):567-76.

Naushad M, Abdullah A, Abdullah Z, Hotan I, Saad M, Mohammed A. Adsorption kinetics, isotherm and reusability studies for the removal of cationic dye from aqueous medium using arginine modified activated carbon. Journal of Molecular Liquids 2019;293:111442.

Oktriyanti M, Palapa NR, Mohadi R, Lesbani A. Modification of Zn-Cr layered double hydroxide with keggin ion. Indonesian Journal of Environmental Management and Sustainability 2019;3(3):93-9.

Palapa NR, Taher T, Rahayu BR, Mohadi R, Rachmat A, Lesbani A. CuAl LDH/rice husk biochar composite for enhanced adsorptive removal of cationic dye from aqueous solution. Bulletin of Chemical Reaction Engineering and Catalysis 2020;15(2):525-37.

Palapa NR, Taher T, Mohadi R, Rachmat A, Lesbani A. Preparation of copper aluminum-biochar composite as adsorbent of malachite green in aqueous solution. Journal of Engineering Science and Technology 2021;16(1):259-74.

Patil NP, Bholay AD, Kapadnis BP, Gaikwad VB. Biodegradation of model azo dye methyl red and other textile dyes by isolate *Bacillus circulans* npp1. Journal of Pure and Applied Microbiology 2016;10(4):2793-800.

Rabie AM, Abukhadra MR, Rady AM, Ahmed SA, Labena A, Mohamed HSH, et al. Instantaneous photocatalytic degradation of malachite green dye under visible light using novel green Co-ZnO/algae composites. Research on Chemical Intermediates 2020;46:1955-73.

Rosa SML, Rehman N, De Miranda MIG, Nachtigall SMB, Bica CID. Chlorine-free extraction of cellulose from rice husk and whisker isolation. Carbohydrate Polymers 2012;87(2):1131-8.

Saini RD. Textile organic dyes: Polluting effects and elimination methods from textile waste water. International Journal of Chemistry Engineering Research 2017;9(1):121-36.

Shakoor S, Nasar A. Removal of methylene blue dye from artificially contaminated water using citrus limetta peel waste as a very low cost adsorbent. Journal of the Taiwan Institute of Chemical Engineers 2016;66:154-63.

Suyanta, Kuncaka A. Utilization of rice husk as raw material in synthesis of mesoporous silicates mcm-41. Indonesian Journal of Chemistry 2011;11(3):279-84.

Thommes M, Kaneko K, Neimark AV, Olivier JP, Rodriguez-Reinoso F, Rouquerol J, et al. Physisorption of gases, with special reference to the evaluation of surface area and pore size distribution (IUPAC technical report). Pure and Applied Chemistry 2015;87(9-10):1051-69.

Vimonses V, Lei S, Jin B, Chow CWK, Saint C. Kinetic study and equilibrium isotherm analysis of Congo red adsorption by clay materials. Chemical Engineering Journal 2009;148 (2-3):354-64.

Vinsiah R, Mohadi R, Lesbani A. Performance of graphite for Congo red and direct orange adsorption. Indonesian Journal of Environmental Management and Sustainability 2020;4: 125-32.

Wang F, Pan Y, Cai P, Guo T, Xiao H. Single and binary adsorption of heavy metal ions from aqueous solutions using sugarcane cellulose-based adsorbent. Bioresource Technology 2017;241:482-90.

Wang Y, Zhu L, Jiang H, Hu F, Shen X. Application of longan shell as non-conventional low-cost adsorbent for the removal of cationic dye from aqueous solution. Spectrochimica Acta Part A: Molecular and Biomolecular Spectroscopy 2016; 159:254-61.

Wijayanti A, Susatyo EB, Kurniawan C. Adsorpsi logam Cr(VI) dan Cu(II) pada tanah dan pengaruh penambahan pupuk organik. Indonesian Journal of Chemical Science 2018;7(3):242-8 (in Indonesian).

Yaseen DA, Scholz M. Textile dye wastewater characteristics and constituents of synthetic effluents: A critical review. International Journal of Environmental Science and Technology 2019;16:1193-226.

Zhu J, He J, Du X, Lu R, Huang L, Ge X. A facile and flexible process of β-cyclodextrin grafted on Fe_3O_4 magnetic nanoparticles and host-guest inclusion studies. Applied Surface Science 2011;257(21):9056-62.

Zhu MX, Li YP, Xie M, Xin HZ. Sorption of an anionic dye by uncalcined and calcined layered double hydroxides: A case study. Journal of Hazardous Materials 2005;120(1-3):163-71.